Potential Use of Indium-111-Labeled Polymorphonuclear Leukocytes for the Detection of Lung Microvascular Injury

Dipak K. Das, Harry Steinberg, Dibyendu Bandyopadhyay and Shlomo Hoory

University of Connecticut School of Medicine, Farmington, Connecticut; and Long Island Jewish-Hillside Medical Center, New Hyde Park, New York

The early stages of microvascular injury are often difficult to detect due to the lack of a suitable marker to assess such an injury. We utilized the well known phenomenon of polymorphonuclear leukocyte (PMN) migration to the microvascular bed as a result of acute inflammatory reactions originating from the damaged cells. A radiotracer technique was developed, employing indium-111-labeled PMN for the detection of microvascular injury induced by hyperoxia. New Zealand white rabbits exposed to either 100% oxygen or air for various intervals of time were injected with indium-111-tropolone or oxine-labeled PMNs. Influx of radioactive PMN into the lung was detected in 72 hr/oxygen-exposed animals using gamma scintigraphic technique. Analysis of dry/wet ratios and histological examinations of the lung biopsies indicated noncardiogenic edema formation at this stage. Mortality was 50% beyond 96 hr/oxygen exposure. Our study thus provided a means to detect early microvascular injury during 72 hr/oxygen-exposure, which was not detectable by any other noninvasive techniques. The use of indium-111-labeled PMN thus appears to be a potentially important tool for the clinical assessment of lung microvascular injury.

J Nucl Med 29:657–662, 1988

The endothelial cells of mammalian lung rapidly manifest many distinct structural and functional alterations as a consequence of microvascular injury. The initial phase of lung injury, which is often associated with enhanced microvascular permeability as a result of altered endothelial functions (*1,2*), is difficult to detect due to the lack of a suitable endothelial marker to assess such an injury. Noncardiogenic pulmonary edema, which is detected clinically by measurements of lung water, is usually a later manifestation of partial destruction of pulmonary endothelium (*3*). The study detailed in this report examined the possibility of using a radiotracer technique employing indium-111-(^{111}In) labeled polymorphonuclear leukocytes (PMNs) for the detection of microvascular injury induced by hyperoxia. The objective of this study was not to explore the mechanism of hyperoxic lung injury, but to examine the possibility of using PMN as a marker for the detection of lung microvascular injury using hyperoxic exposure model. The experiment is predicated on the fact that the initial events of certain lung injury may be associated with the loss of thromboresistance which results in the adherence of activated PMNs to the pulmonary microvascular bed (*4,5*). Although controversies exist regarding a direct role of PMNs in oxidative lung injury, an influx of PMNs into the lung area has been observed by all investigators (*4–7*). Our study utilized this phenomenon, and scintigraphy provided a means of identifying the ongoing accumulation of indium-111-labeled PMNs in the lung.

Received June 5, 1987; revision accepted Nov. 24, 1987.

For reprints contact: Dipak K. Das, PhD, Cardiovascular Laboratories, University of Connecticut School of Medicine, Farmington, Connecticut 06032.

MATERIALS AND METHODS

Oxygen Exposure

New Zealand white rabbits were exposed to 95–98% oxygen for various intervals of time in a Plexiglas chamber (*8*). O_2 flow rates were maintained to ensure concentrating turnover of chamber gas three to five times per hour. The chamber temperature was maintained at 25–27°C. Control rabbits were simultaneously exposed to air using the same time frame as experimental rabbits.

PMN Labeling

Whole blood was collected from human volunteers in acid citrate dextrose (5:1, v/v). The PMNs were isolated by one-

step density centrifugation technique using mono-poly resolving medium (Flow Laboratories, NY), as described previously (*9*). Sixty to eighty microcuries each of [^{111}In]tropolone or [^{111}In]oxine (Mediphysics, CA) were incubated with PMNs (3×10^6) in Hanks balanced salt solution containing Hepes buffer at pH 7.4, 37°C for 20 min (*9,22*). These labeled PMNs were divided into two parts and infused into both the oxygen-exposed and air-exposed rabbits. Control experiments consisting of air-exposed rabbits were simultaneously performed at each time level along with experiment groups containing O_2-exposed animals.

Viability and Chemotaxis

The cell viability was determined by the trypan blue dye exclusion method. Chemotaxis was assessed using a modified Boydens Chamber method (*10*) employing zymogen activated serum as the chemoattractant. The leading from method was used to evaluate cell migration.

In vivo neutrophil viability was assessed by making one-half inch incisions in both hind legs of the animals under aseptic conditions. In one of the legs, polyvinyl sponges containing 1 μM endotoxin were implanted in the subcutaneous tissue, as described previously (*11*). The other hind leg received sponges treated with normal saline. Twenty-four hours after treatment, the rabbits were injected with about 2.96 MBq (80 μCi) of either [^{111}In]tropolone or [^{111}In]oxine labeled with human PMNs. Imaging was performed both at 4 and 24 hr, and sponges were counted simultaneously for accumulated PMNs.

Although control experiments with air-exposed rabbits were simultaneously performed at each time period along with the experimental groups involving O_2-exposed animals, both biodistribution of ^{111}In radioactivity and scintigraphy showed the same results for all the control groups, suggesting that the duration of air-exposure has no effect on PMN-influx into the lung. Therefore, we combined all the control groups from 24 hr, 48 hr, 72 hr, and 96 hr air-exposed animals and showed them as one unified control group.

Gamma Scintigraphy

Uptake and turnover of ^{111}In-labeled PMNs were monitored by gamma scintigraphy at 4 hr and 24 hr postinjection of radiolabeled PMNs into the rabbits. The camera (Siemen's large field-of-view gamma scintillation camera, ZLC-750) was linked to a Vax 11-750 minicomputer that controlled the acquisition and stored all images. A medium-energy, parallel hole collimator was used that had a resolution of better than 4 mm at the camera face. The camera was set with 20% window to accept both photopeaks of ^{111}In of 173 keV and 247 keV energies. Images were digitized in a 64 × 64 matrix, and various regions of interest in lung, liver, and kidney were studied.

Tissue Processing

Rabbits were killed following imaging, and vital organs including lung, liver, and kidney were collected and counted for radioactivity in a well counter. Lung injury was assessed by evaluating dry/wet weight ratios, and light and transmission electron microscopy.

Statistical Analysis

Statistical analysis of the data was made by means of a one-way analysis of variance. Comparisons among individual groups were made by a t-test using the pooled variance from the analysis of variance.

RESULTS

Neutrophil Viability and Chemotaxis

Data from viability and chemotaxis are shown in Table 1. Cell viability as evidenced by the vital dye exclusion method was found to be excellent (>98%) at every stage of the labeling procedure. The chemotactic response of the PMNs was read directly from the optical micrometer attached to the fine focusing knob of the microscope. The values were essentially identical for labeled and unlabeled cells. Labeling efficiency for oxine was 91.0 ± 1.2% compared to that of tropolone of 96.3 ± 2.5%.

Indium-111-labeled PMNs were also able to migrate to a known inflammatory stimulus. Squeezate from the endotoxin-treated sponges contained >90% PMNs. The number of counts per PMN in the squeezate compared favorably with that of circulating PMN counts immediately after the incision. Plasma containing ^{111}In label accounted for only 5% of the total [^{111}In]PMN radioactive counts in the sponge. Scintigraphy, performed

TABLE 1
Functional Characteristics of PMNs Labeled with [^{111}In]Tropolone or Oxine*

Test type	Before labeling	After labeling		p-Value
		[^{111}In]oxine	[^{111}In]tropolone	
Viability (n = 25)	98.6 ± 0.5%	98.1 ± 0.9%	98.2 ± 0.8%	N.S.
Chemotaxis	97.2 ± 9.3 μm	92.8 ± 5.9 μm	90.4 ± 8.4 μm	N.S.
In vivo chemotaxis				
Sponge squeezate (PMN as % of total cells) (n = 3)	—	>90%	>90%	
Scintigraphy (sponge implanted area/muscle background ratio per pixel) (n = 3)	—	8.95 ± 1.21	9.53 ± 2.09	

* Results are expressed as mean ± s.e. of indicated number (n) of separate experiments. In vivo chemotaxis experiments for alpha-scintigraphy and sponge squeezate counting were performed after 24 hr following PMN injection.

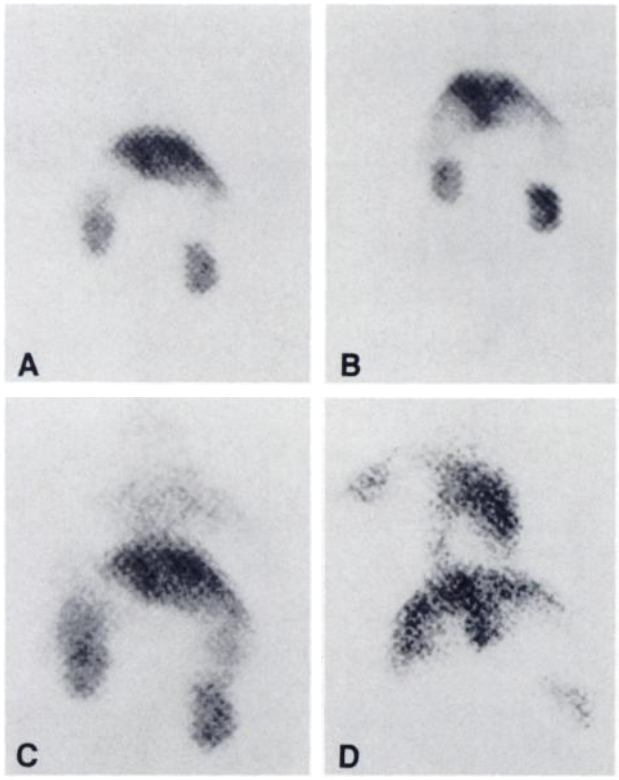

FIGURE 1
Scintigraphy of rabbits under gamma camera. PMNs labeled with [^{111}In]oxine were infused after 24 (A), 48 (B), 72 (C), and 96 (D) hr of oxygen exposure, and scintigraphic imaging was performed 4 hr postinjection.

prior to removing the implanted sponges, also showed localization of the radioactivity in the inflammatory regions of the hind leg.

Gamma Scintigraphy

Localization of radioactivity (4 hr and 24 hr post injection) was observed in the lung area of 72 hr and 96 hr oxygen-exposed animals, whereas minimal or no localization was detected in 24 hr and 48 hr exposed or control animals (Fig. 1). Both [^{111}In]oxine and [^{111}In] tropolone showed similar results, but the latter agent showed some activity in the kidney region during 4 hr acquisition. Twenty-four-hour postinjection ([^{111}In] tropolone PMN) scintigraphy, however, showed diminished activity in the kidney, although localization in the lung area remained.

Computer-generated regions of interest were established for each vital organ in all images. The data after 4 hr of PMN injection showed that average counts per pixel in lungs where PMNs were labeled with [^{111}In] tropolone were twice that of the lungs where PMNs were labeled with [^{111}In]oxine (Table 2). Clearance rate of tropolone-indium was, however, higher compared to oxine-indium, such that after 24 hr the activities of both indium and tropolone were identical (data not shown). Backgrounds were chosen in the adjacent areas around the lung, liver and kidney, and an average of the counts of these regions were used. Each view was acquired for a preset count of 250,000, which usually occurred between 10–15 min depending on the amount of radioactivity administered. To eliminate errors resulting from the tissue distribution, we also evaluated scintigrams of other organs and found no significant differences in counts per pixel. Localization of radioactivity was observed in both 72 hr and 96 hr oxygen-exposed animals compared to controls ($p < 0.01$).

Biodistribution of Indium-111 Radioactivity

Influx of radioactive PMNs was confirmed by counting the radioactivity incorporated in lung and other tissues after sacrificing the animals. The radioactivity incorporated into lungs of tropolone-PMN animals was somewhat higher compared to that of oxine-PMN animals. A significantly higher amount of radioactivity was found in the lung biopsies from 72 and 96 hr oxygen-exposed animals ($p < 0.005$ compared to controls). In

TABLE 2
Scintigraphic Comparison of Radioactivity Accumulation in Lung, Liver, and Kidney During Hyperoxic Exposure

Duration of oxygen exposure	Scintigrams (Organ/Background ratio per pixel)					
	Lung		Liver		Kidney	
	Oxine	Tropol	Oxine	Tropol	Oxine	Tropol
Control (oxine n = 5)	1.95	3.35	3.58	4.02	3.50	4.42
(tropol n = 8)	±0.39	±0.41	±0.62	±0.36	±0.29	±0.16
24 hr (tropol n = 6)	—	3.41	—	3.66	—	4.61
		±0.23	—	±0.47		±0.18
48 hr (oxine n = 4)	1.86	3.69	3.62	3.97	3.38	4.75
(tropol n = 5)	±0.37	±0.50	±0.45	±0.45	±0.33	±0.20
72 hr (oxine n = 8)	3.88*	6.85*	3.40	3.51	3.66	4.58
(tropol n = 17)	±0.65	±0.78	±0.29	±0.50	±0.24	±0.15
96 hr (oxine n = 7)	6.59*	8.37*	4.16	4.15	3.98	4.48
(tropol n = 14)	±0.81	±0.21	±0.77	±0.62	±0.34	±0.25

* $p < 0.005$ compared to controls.
Results are expressed as mean ± s.e. of indicated number (n) of separate experiments.

liver and kidney, no significant differences in radioactivity were observed (Table 3).

Dry/Wet Weight Ratios

Lung injury was evaluated by estimating dry/wet weight ratios. Dry/wet weight ratios increased appreciably after 96 hr exposure, although some increase was also noticed after 72 hr of oxygen exposure (Table 4).

Histologic Evaluations

Histologic examinations of the lung biopsies from the control as well as 24 hr or 48 hr oxygen-exposed rabbits demonstrated little to no interstitial edema (Fig. 2A). In the 72 hr oxygen-exposed rabbit lungs, there was histologic evidence of some interstitial edema (Fig. 2B) which increased significantly, leading to gross cytoplasmic edema formation in 96 hr exposed animals (Fig. 2C).

TABLE 4
Comparisons of Lung Dry/Wet Wt Ratios During Hyperoxic Exposure

Duration of oxygen exposure	Dry wt / Wet wt
Control (n = 12)	0.19 ±0.02
24 hr (n = 6)	0.19 ±0.01
48 hr (n = 9)	0.18 ±0.02
72 hr (n = 25)	0.16* ±0.01
96 hr (n = 21)	0.13* ±0.02

*$p < 0.005$ compared to controls.
Results are expressed as mean ± s.e. of the indicated number (n) of separate experiments.

DISCUSSION

This study warrants the use of ^{111}In-labeled PMNs as imaging agent for noninvasive detection of the early stages of microvascular injury. In our study, 72 hr oxygen-exposed rabbits showed evidences of pulmonary microvascular endothelium injury only when evaluated by noninvasive techniques such as histological examinations and edema formations from lung biopsies. Nevertheless, ^{111}In-labeled PMNs detected the lung injury at this stage as evidenced by localization of radioactivity in the damaged area by gamma scintigraphy.

Recent studies indicated the importance of PMNs in the development of varieties of lung injury, including endothelial damage and edema formation (*4–7,12–14*). Other studies, on the other hand, demonstrated pulmonary injury even in the complete absence of PMN (*4,15,16*). Although the exact role of PMN in the development of microvascular injury is speculative, the migration of PMN in the damaged area is a well known phenomenon. The early features of hyperoxic injury include intravascular activation of complement accumulation of granulocytes in the postcapillary venule region of the adjacent microvasculature of the pulmonary microcirculation with subsequent edema formation, although complement or neutrophils may not play a primary role in the development of pulmonary oxygen toxicity. This, in turn, might cause the migration of PMN through the endothelial gaps across the vascular wall. The chemotactic factor-induced margination of PMN probably produces a vasopermeability mediator, resulting in protein exudation and swelling of the tissue observed in many instances (*17,18*). The formation of edema during continued hyperoxic exposure, presumably due to an increase in the permeability of pulmonary capillaries and histologic evidence of capillary damage in oxygen-poisoned lungs, supports this mech-

TABLE 3
Comparison of Biodistribution of ^{111}In Radioactivity During Hyperoxic Exposure

Duration of oxygen exposure	Indium-111 activity (% Injected dose/g) Lung		Liver		Kidney	
	Oxine	Tropol	Oxine	Tropol	Oxine	Tropol
Control (oxine n = 5) (tropol n = 8)	2.5 ±2.0	2.9 ±2.1	0.56 ±0.02	0.50 ±0.08	0.73 ±0.09	1.40 ±0.11
24 hr (tropol n = 6)	—	2.2 ±0.52	—	0.61 ±0.05	—	1.51 ±0.15
48 hr (oxine n = 4) (tropol n = 5)	3.2 ±1.9	2.5 ±1.7	0.38 ±0.04	0.53 ±0.02	0.99 ±0.07	1.38 ±0.10
72 hr (oxine n = 8) (tropol n = 17)	7.2* ±2.9	9.7* ±4.1	0.59 ±0.04	0.58 ±0.08	0.78 ±0.24	1.72 ±0.16
96 hr (oxine n = 7) (tropol n = 14)	10.5* ±2.0	12.0* ±0.7	0.79 ±0.05	0.65 ±0.07	0.25 ±0.31	1.56 ±0.24

*$p < 0.005$ compared to controls.
Results are expressed as mean ± s.e. of indicated number (n) of separate experiments.

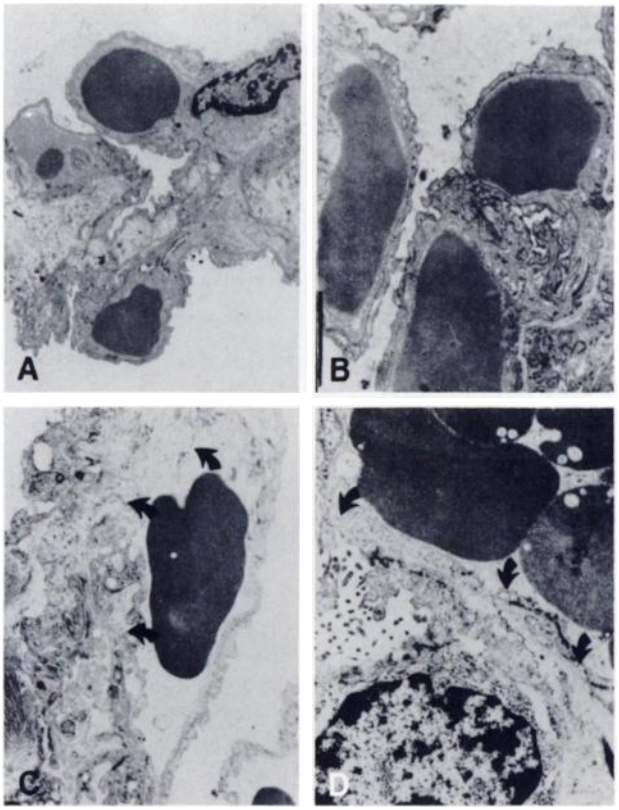

FIGURE 2
Transmission electron microscopy of lung biopsies from rabbits exposed to oxygen for 24 (A), 48 (B), 72 (C), and 96 (D) hours. Figures A and B show intact endothelial lining, whereas Figures C and D demonstrate considerable interstitial edema secondary to loss of endothelial integrity (arrow).

anism (*19*). Prolonged exposure to 100% oxygen finally leads to increased lung weight, pulmonary damage terminating in hypoxemia, acidosis, and death (*20,21*).

We have used PMNs isolated from human blood, because human blood yields a greater number of PMNs compared to those obtained from rabbit blood. We have recently characterized ^{111}In-labeled human PMNs, which have been used to study in vivo chemotaxis in rabbits (*22*). We did not find any differences in physiological functions using human PMNs in rabbits. The circulating half-lives of PMNs and kinetic studies have been described elsewhere (*23*).

We have used both [^{111}In]oxine and [^{111}In]tropolone as binding agents with PMNs. At the present time, complexes of [^{111}In]oxine have found wide acceptance as labeling agents for white blood cells. This agent is alcohol soluble and is always the subject of concern regarding the ultimate viability of the prepared cells. The water-soluble metal chelate [^{111}In]tropolone, on the other hand, being five times as lipid-soluble as [^{111}In] oxine, can be incorporated into the cell with high efficiency. Since the incorporation of the cell into the damaged lung was of prime concern, we used both the compounds to examine the relative efficacy of using oxine versus tropolone as the binding agent.

The results of our study, however, indicated that [^{111}In]tropolone behaves similarly to [^{111}In]oxine as an imaging agent in evaluating PMN influx into lung and in assessing the microvascular injury. The relatively higher amount of PMN influx into the lung with [^{111}In] tropolone compared to [^{111}In]oxine may be explained by the enhanced lipid cytobility and efficient labeling in acid citrate dextrose of [^{111}In]tropolone as reported earlier (*22*).

In our study, injury to pulmonary microvascular endothelium appeared to occur after 48 hr of oxygen exposure, which was detected by scintigraphic technique. This injury is presumably an early and critical event in the development of a variety of diffuse lung injuries. Unfortunately, there is no noninvasive technique available to detect such an early event of lung injury. Blood gas analysis did not show any abnormality in 72 hr oxygen-exposed rabbits. However, injury to pulmonary microvascular endothelium was obvious by histological examinations at this stage. Noncardiogenic pulmonary edema formation was also confirmed by the dry/wet weight ratios of the lung biopsies. Clinically detectable edema occurred after 96 hr oxygen exposure when the microvascular injury advanced to a critical stage. In our study, we found only 50% mortality beyond 96 hr oxygen exposure.

Several tests are currently available to detect noncardiogenic edema formation, although none of them appears to be of great significance in detecting early microvascular injury. Measurement of extravascular lung water by the thermal green dye technique has been used by some investigators to detect edema formation, although this technique may give rise in erroneous results because of the modified surface area of the pulmonary microvascular exchanging membrane. Radiotracers injected into the vascular system, in conjunction with indicator dilution techniques, have been used to detect microvascular permeability and extravascular lung water content. The measurement of permeability-surface area with carbon-14 urea has been used successfully to detect extravascular lung water. Use of inhaled radiotracer such as technetium-99m diethylenetriaminepentaaceate has also been reported to detect cardiogenic and noncardiogenic forms of edema.

The above studies, although not difficult to perform, require adequate clinical experience and controlled conditions to achieve success. In addition, these methods can only detect the noncardiogenic edema, which is a later manifestation of undetectable early microvascular injury. The methods described in our studies are routinely performed in departments of nuclear medicine of many institutions and hospitals to detect abscess formation. The study is very simple, and isolation of PMN and cell labeling can be achieved within a very

short period of time, usually within 2 hr. In our studies, 4 hr postinjection of labeled PMN imaging showed excellent results. There is a definite need for new approaches to the clinical assessment of lung microvascular injury, and to this end, use of ^{111}In-labeled PMNs appears to be highly promising and worth pursuing.

ACKNOWLEDGMENTS

This study was partially supported by grants from the American Heart Association (Nassau Chapter), the American Heart Association Connecticut Affiliate, NIH HL 33801, and NIH HL 34360. Mrs. Joanne D'Aprile provided excellent secretarial assistance.

REFERENCES

1. Steinberg H, Greenwald RA, Sciubba J, et al. The effect of oxygen-derived free radicals on pulmonary endothelial cell function in the isolated perfused rat lung. *Exp Lung Res* 1982; 3:163–173.
2. Block ER, Fisher AB. Depression of serotonin clearance by rat lung during oxygen exposure. *J Appl Physiol* 1977; 42:33–38.
3. Crapo JD, Barry BE, Foscue HA, et al. Structural and biochemical changes in rat lungs occurring during exposure to lethal and adaptive doses of oxygen. *Am Rev Respir Dis* 1980; 122:123–143.
4. Bowman CM, Butler EN, Repine JE. Hyperoxia damages cultured endothelial cells causing increased neutrophil adherence. *Am Rev Respir Dis* 1983; 128:469–472.
5. Shasby DM, Shasby SS, Peach MJ. Granulocytes and phorbol myristate acetate increase permeability to albumin of cultured endothelial monolayers and isolated perfused lungs. *Am Rev Respir Dis* 1983; 127:72–76.
6. Flick MR, Perel A, Staub NC. Leukocytes are required for increased lung microvascular permeability after microembolization in sheep. *Circ Res* 1981; 48:344–351.
7. Till GO, Johnson KJ, Kunkel R, et al. Intravascular activation of complement and acute lung injury. *J Clin Invest* 1982; 69:1126–1135.
8. Steinberg H, Greenwald RA, Moak SA, et al. The effect of oxygen adaptation on oxyradical injury to pulmonary endothelium. *Am Rev Respir Dis* 1983; 128:94–97.
9. Bandyopadhyay D, Levy LM, Schiff R, et al. Rapid in vitro labeling of polymorphonuclear leukocytes with indium-111-tropolone. *J Nucl Med* 1983; 24:7.
10. Zigmond SH, Hirsh JG. Leukocyte locomotion and chemotaxis. New methods for evaluation and demonstration of cell-derived chemotactic factor. *J Exp Med* 1973; 137:387–410.
11. Steinberg H, Neogi A, Mandelbaum S, et al. Neutrophil kinetics in oxygen toxicity. In: *Oxyradicals and their scavenger systems, Vol II.* New York: Elsevier Science Publishing Co., Inc., 1983:375–378.
12. Craddock PR, Fehr J, Brigham KL, et al. Complement and leukocyte-mediated pulmonary dysfunction in hemodialysis. *N Engl J Med* 1977; 296:769–774.
13. Heflin AC, Brigham KL. Prevention by granulocyte depletion of increased vascular permeability of sheep lung following endotoxemia. *J Clin Invest* 1981; 68:1253–1260.
14. Johnson A, Malik AB. Pulmonary edema after glass bead microembolization: protective effect of granulocytopenia. *J Appl Physiol* 1982; 52:155–161.
15. Martin WJ II, Gadek JE, Hunninghake GW, et al. Oxidant injury of lung parenchymal cells. *J Clin Invest* 1981; 68:1277–1288.
16. Usha Raj J, Hazinski TA, Bland RD. Oxygen-induced lung microvascular injury in neutropenic rabbits and lambs. *J Appl Physiol* 1985; 58:921–927.
17. Frank L, Massaro D. Oxygen toxicity. *Am J Med* 1980; 69:117–126.
18. Kistler GS, Caldwell PRB, Weibel ER. Development of fine structural damage to alveolar and capillary lining cells in oxygen-poisoned rat lungs. *J Cell Biol* 1967; 32:605–628.
19. Kapanci Y, Weibel ER, Kaplan HP, et al. Pathogenesis and reversibility of the pulmonary lesions of oxygen toxicity in monkeys. II. Ultrastructural and morphometric studies. *Lab Invest* 1969; 20:101–118.
20. Kaplan HP, Robinson FR, Kapanci Y, et al. Pathogenesis and reversibility of the pulmonary lesions of oxygen toxicity in monkeys. I. Clinical and light microscopic studies. *Lab Invest* 1969; 20:94–100.
21. Smith CW, Lehan PH, Monks JJ. Cardiopulmonary manifestations with high O_2 tensions at atmospheric pressure. *J Appl Physiol* 1963; 18:849–853.
22. Bandyopadhyay D, Schiff RG, Hoory S, et al. ^{111}Indium-tropolone labeled human PMNs: a rapid method of preparation and evaluation of labeling parameters. *Inflammation* 1987; 11:13–22.
23. Steinberg H, Das DK, Cerreta JM, et al. Neutrophil kinetics in O_2-exposed rabbits. *J Appl Physiol* 1986; 61:775–779.